BMC Plant Biology

RESEARCH Open Access

Identification of a key gene involved in triterpenoid biosynthesis in *Sanghuangporus baumii* under Mn^{2+} induction and its regulatory role

Zengcai Liu[1], Chenyuan Si[1], Wenqi Xiao[1], Anxin Wang[1] and Li Zou[1*]

Abstract

Background Triterpenoids derived from *Sanghuangporus baumii* exhibit significant pharmacological activities. However, their production remains limited due to the naturally low yield of triterpenoids and insufficient knowledge of the biosynthetic pathway.

Results *S. baumii* strain DL102 was isolated, and the effects of Mn^{2+} on its mycelial growth and metabolism were assessed. Treatment with 1 mM Mn^{2+} significantly enhanced mycelial biomass accumulation, increasing by 0.42 g/L compared to the Mn0 group. This increase was associated with enhanced soluble sugar content and the upregulation of the expression of key metabolic genes. Furthermore, total triterpenoids content peaked at 10 mM Mn^{2+} (28.7 ± 0.3 mg/g), representing a 2.03-fold increase relative to the Mn0 control group. This enhancement was primarily attributed to the activation of the terpenoid biosynthesis pathway, particularly through *HMGS* (3-hydroxy-3-methylglutaryl-CoA synthase) regulation by Mn^{2+}. The heterologous expression of *HMGS* in *Saccharomyces cerevisiae* resulted in the overexpression strain Sc-HS1, which exhibited significantly higher squalene production compared to the Ck strain, regardless of the presence or absence of an inducer.

Conclusions Our findings highlight the critical role of *HMGS* in triterpenoid biosynthesis under Mn^{2+} treatment. These data provide a foundation for optimizing triterpenoids production, with potential applications in industrial-scale bioprocessing.

Keywords *Sanghuangporus baumii*, Manganese, Biomass, Soluble sugar, Triterpenoids, *HMGS*

*Correspondence:
Li Zou
shyj@nefu.edu.cn
[1]College of Forestry, Northeast Forestry University, Harbin 150040, China

Background

Syringa reticulata is a deciduous tree with recognized medicinal properties and is parasitized by the macrofungus *Sanghuangporus baumii* [1, 2]. *S. baumii* has demonstrated significant medicinal potential, including antitumor [3], antioxidant [4], and hypoglycemic [5] effects. Various pharmacologically active compounds have been identified in *S. baumii*, such as triterpenoids, polysaccharides, and polyphenols [6], with triterpenoids being recognized as the key bioactive components responsible for its therapeutic efficacy [7, 8]. However, the naturally low yield of triterpenoids, combined with the limited availability of wild resources, severely restricts their pharmacological applications [9]. Enhancing their production in *S. baumii* is therefore of great importance, yet remains a significant challenge due to their complex structures and the limited understanding of pertinent biosynthetic pathways.

Although certain structurally simple terpene skeletons and diterpene canataxpropellane can be chemically synthesized with relative ease, the synthesis of triterpenoids is more challenging and time-consuming due to structural diversity and complexity [10, 11]. In contrast, biosynthesis has emerged as a promising alternative due to its environmentally friendly nature and potential for yield improvement [12, 13]. In macrofungi, triterpenoids are primarily synthesized via the mevalonate pathway, which involves multiple catalytic and modification steps regulated by key genes. Identifying these genes is essential for enhancing triterpenoid biosynthesis [14]. For instance, Ren et al. [15] demonstrated that adding exogenous inducer (Methyl jasmonate) increased total triterpenoids content by 45.3% in *Ganoderma lucidum*, likely by upregulating the expression of the key gene *HMGS*. Subsequent cloning and heterologous expression of this gene in yeast confirmed its catalytic function [16]. In addition, Zhang et al. [17] cloned the *IDI*, *FPPS*, and *SQS* genes, whose overexpression led to a 49-fold increase in triterpenoid (β-amyrin) production in *Saccharomyces cerevisiae*. Collectively, these findings highlight the potential of yeast-based metabolic platforms for gene identification and efficient heterologous triterpenoids production.

Manganese (Mn^{2+}) has been identified as an effective inducer for enhancing triterpenoids content and regulating key genes [18]. At present, no studies have reported the effects of Mn^{2+} induction on triterpenoid biosynthesis in *S. baumii*. In this study, we treated *S. baumii* mycelia with Mn^{2+} and analyzed changes in biomass and total triterpenoids content. Transcriptome analysis was performed to identify potential metabolic pathways and key regulatory genes involved in Mn^{2+}-mediated triterpenoid biosynthesis. The regulatory function of a key gene (*HMGS*) was further verified through heterologous expression. Our findings provide valuable insights for optimizing *S. baumii* triterpenoids production.

Results

Effects of Mn^{2+} on *S. baumii* mycelial growth and triterpenoid biosynthesis

S. baumii fruiting body is fan-shaped, with a rough surface displaying concentric rings and cracks, and varies in color from yellow–brown to dark black (Fig. 1a). Mycelia obtained via tissue isolation appeared white to yellow (Fig. 1b). PCR amplification of the ITS (Universal DNA barcode for identifying fungi) region generated a product of approximately 770 bp for both the fruiting body (PX054576) and mycelia (Fig. 1c, Table S1). BLAST analysis confirmed the identity of the strain as *S. baumii* (Fig. S1), designated as strain DL102.

Treating *S. baumii* mycelia with varying concentrations of Mn^{2+} induced metabolic changes, as evidenced by a significant darkening of the fermentation broth compared to the Mn0 control group (Fig. 1d). Mn^{2+} exposure also affected mycelial biomass, with the highest biomass observed in the Mn1 group (4.46 ± 0.04 g/L), representing a 0.42 g/L increase relative to the Mn0 group. However, Mn^{2+} concentrations of ≥ 5 mM significantly inhibited biomass accumulation (Fig. 1e). Moreover, total triterpenoids content increased in a concentration-dependent manner upon Mn^{2+} treatment, reaching a maximum at 10 mM Mn^{2+} (28.7 ± 0.3 mg/g; DCW, dry cell weight), which was 2.03 times higher than that in the Mn0 group (Fig. 1f). These results indicate that Mn^{2+} plays a significant role in both *S. baumii* mycelial growth and triterpenoid biosynthesis.

Effects of Mn^{2+} on metabolic pathways and DEGs

Transcriptome analysis was performed using the significant differences in triterpenoids content among *S. baumii* samples treated with Mn^{2+} (Mn0, Mn1, and Mn10 groups). Sequencing data from nine samples showed sufficient saturation (Fig. S2) and high quality, with Q20 and Q30 values exceeding 98.66% and 96.07%, respectively (Table S2). PCA confirmed high reproducibility within the three groups (Fig. 2a). Hierarchical clustering demonstrated strong repeatability across samples, with Mn^{2+}-treated samples (Mn1 and Mn10 groups) clustering together and exhibiting significant DEGs (Fig. 2b).

Differential gene analysis identified 1,596 DEGs (838 up- and 758 downregulated) between the Mn0 and Mn1 groups, 2,624 DEGs (1,143 up- and 1,481 downregulated) between the Mn0 and Mn10 groups, and 1,258 DEGs (580 up- and 678 downregulated) between the Mn1 and Mn10 groups (Fig. 2c). Relative expression levels of nine DEGs, as validated by qRT-PCR, were consistent with corresponding FPKM values (Fig. 2d, Table S3). KEGG enrichment analysis identified significant enrichment of

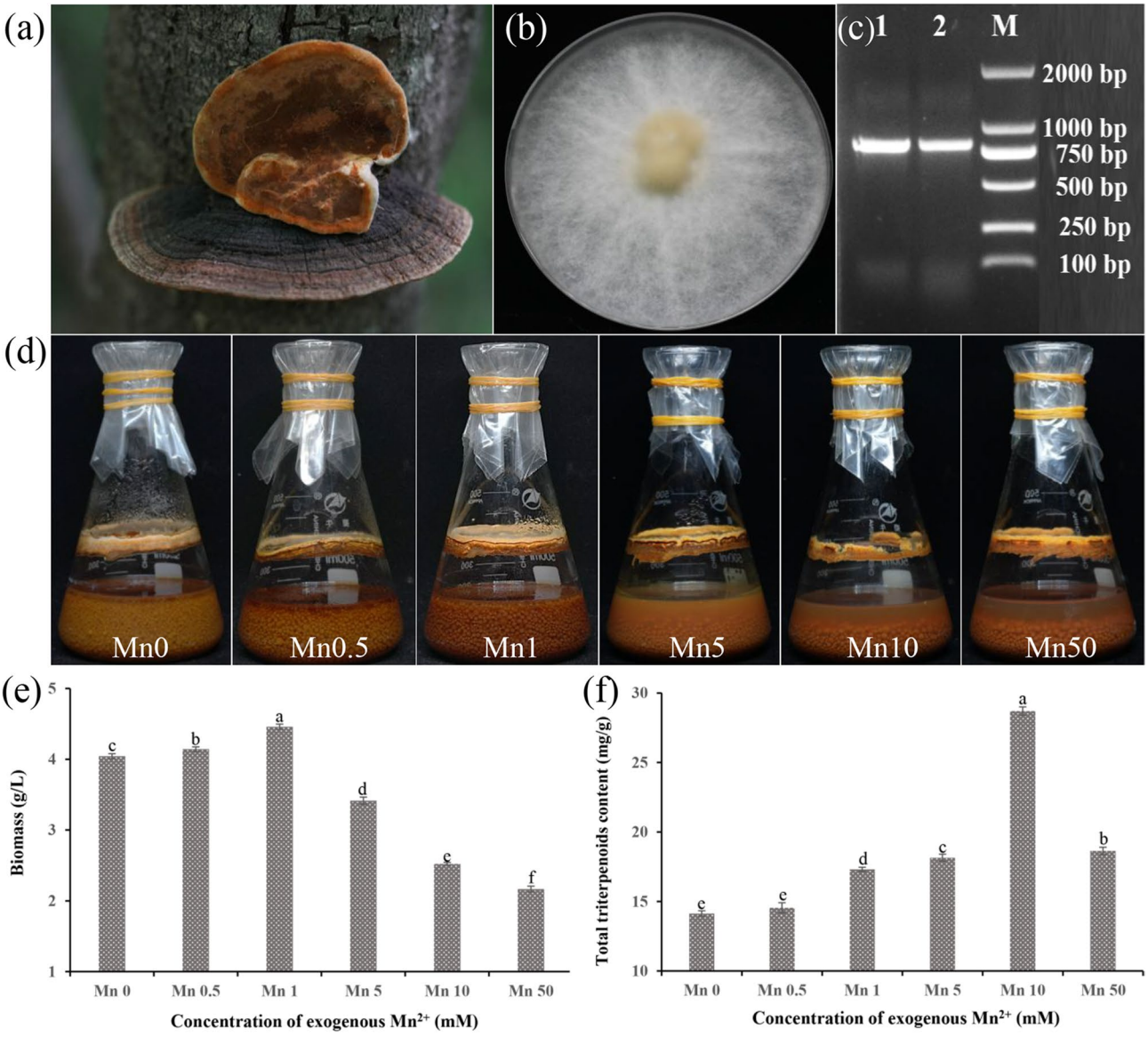

Fig. 1 Effects of Mn^{2+} on *S. baumii* growth and metabolism. **a** *S. baumii* fruiting body. **b** *S. baumii* mycelia. **c** PCR amplification of the ITS region: 1, fruiting body; 2, mycelia; M, marker 2000. **d** Fermentation culture of *S. baumii* mycelia treated with Mn^{2+}. **e** Biomass accumulation. **f** Total triterpenoids content

pathways related to starch and sucrose metabolism, peroxisome function, pyruvate metabolism, and terpenoid backbone biosynthesis, suggesting their involvement in Mn^{2+}-induced metabolic and growth changes in *S. baumii* (Fig. 2e).

DEG analysis and key gene identification in triterpenoid biosynthesis

Triterpenoid biosynthesis was obviously upregulated in Mn^{2+}-treated *S. baumii*, with *PDH1* expression and acetyl-CoA content (158.65 nmol/g) showing an increase in the Mn10 group (2.21- and 2.63-fold higher than those in the Mn0 group, respectively). Expression levels of nine triterpenoid biosynthesis-related genes (*AACT*, *HMGS*, *HMGR*, *MVK*, *PMK*, *MVD*, *IDI*, *FPPS*, and *SQS)* also steadily increased with Mn^{2+} concentrations, driving continuous catalytic production of triterpenoids from acetyl-CoA via the terpenoid backbone biosynthesis pathway (Fig. 3a). Pearson correlation analysis identified *AACT*, *HMGS*, *HMGR*, *PMK*, and *IDI* as highly correlated with triterpenoid biosynthesis ($R > 0.90$; Fig. 3b). Notably, *HMGS* exhibited a 26-fold increase, suggesting its pivotal role in Mn^{2+}-mediated regulation of triterpenoid biosynthesis in *S. baumii* (Table S3).

Cloning and functional verification of *HMGS*

HMGS was cloned using pYE-HMGS primers, yielding a 1,520 bp product (Fig. 4a). This gene encodes a 495

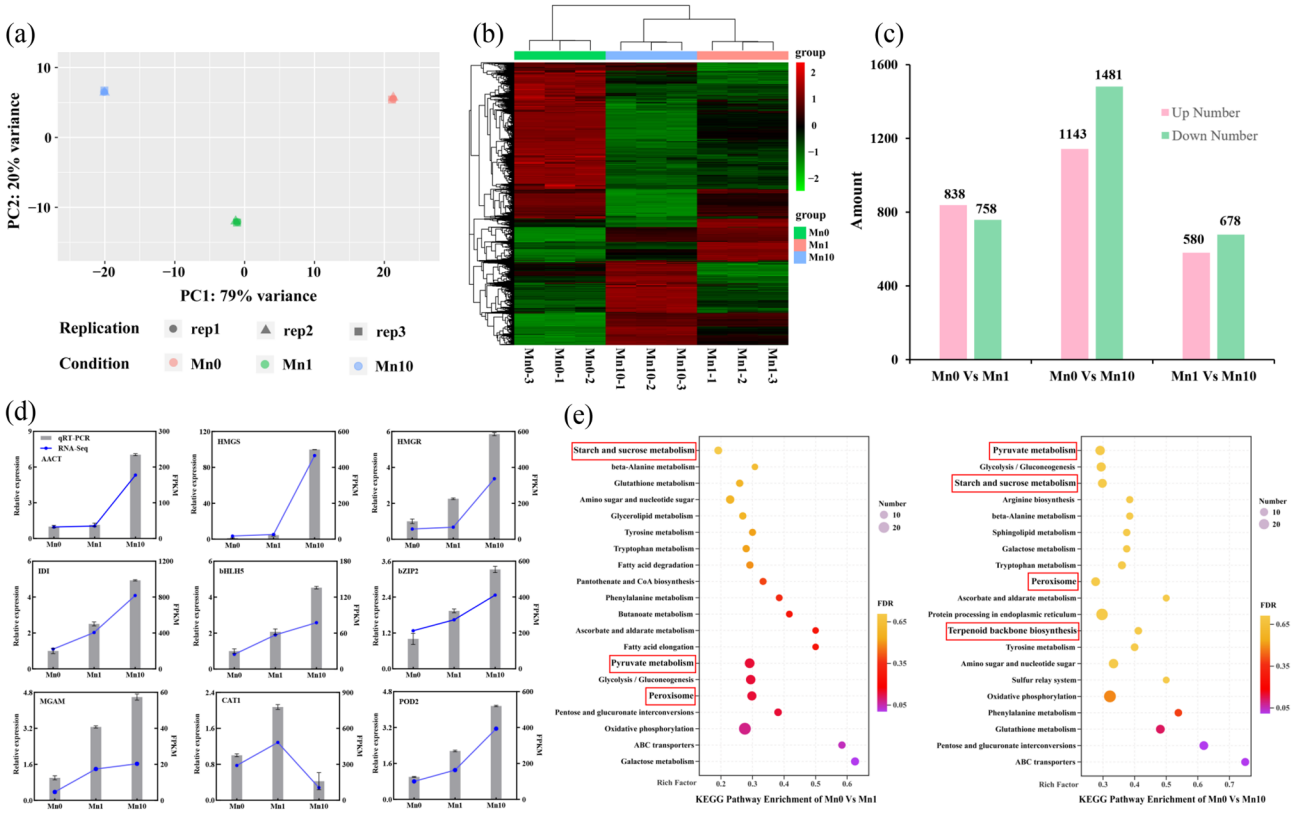

Fig. 2 Transcriptome analysis of metabolic changes in *S. baumii* treated with different Mn^{2+} concentrations. **a** PCA score plot of transcriptomic profiles from the Mn0, Mn1, and Mn10 groups. **b** Clustering analysis of gene expression patterns across the Mn0, Mn1, and Mn10 groups. **c** DEGs identified through pairwise comparisons among the three groups, showing up- and downregulated genes. **d** Comparison of gene expression levels from qRT-PCR and transcriptomic data. **e** KEGG pathway enrichment analysis of DEGs from pairwise comparisons

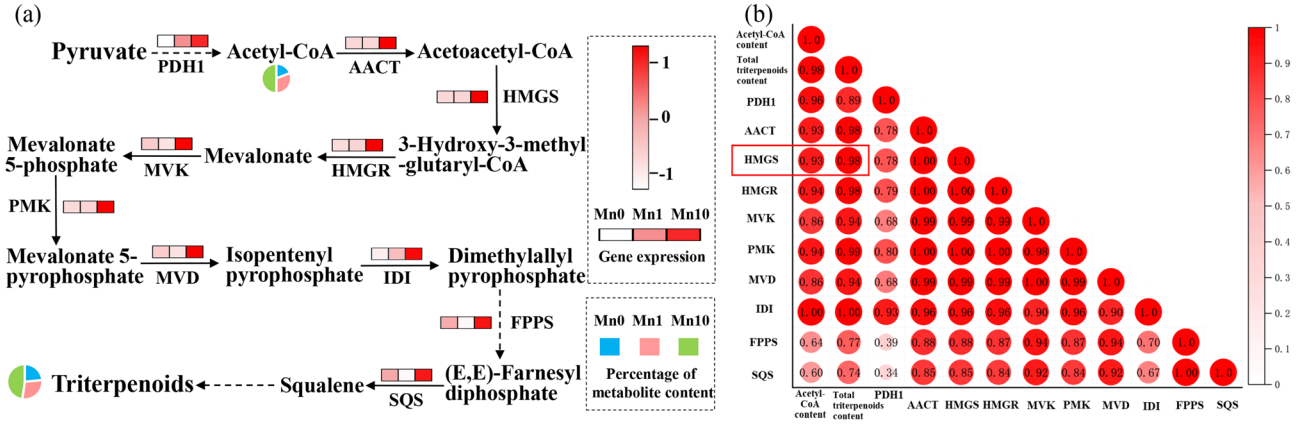

Fig. 3 Effects of Mn^{2+} on triterpenoid biosynthesis in *S. baumii*. pyruvate dehydrogenase, PDH; acetyl-CoA acyltransferase, AACT; 3-hydroxy-3-methylglutaryl-CoA synthase, HMGS; 3-hydroxy-3-methylglutaryl-CoA reductase, HMGR; mevalonate kinase, MVK; phosphomevalonate kinase, PMK; mevalonate pyrophosphate decarboxylase, MVD; isopentenyl diphosphate isomerase, IDI; farnesyl diphosphate synthase, FPPS; squalene synthase, SQS. **a** Gene expression levels and metabolites content. **b** Pearson correlation analysis between gene expression levels and acetyl-CoA/total triterpenoids content

amino acid protein with a conserved HMG-CoA-S_euk structural domain (Fig. S3; PX056318) and highly conserved amino acid residues, including Glu-108, Tyr-143, His-294, Asn-373, and Ser-407 (Fig. 4b). To assess the function of *HMGS* in triterpenoid biosynthesis, *HMGS* was inserted into the pYES2-ntc vector to generate pYES2-HMGS (Fig. 4c) and subsequently expressed in *S. cerevisiae*. Positive transformants (Sc-HS1) were confirmed through PCR (T7F/C1R primers, approximately 1,800 bp product; Fig. 4d). Squalene content in Sc-HS1 (1.13 ± 0.01 mg/L) was 1.92-fold higher than the Ck group (0.59 ± 0.03 mg/L, Fig. 4e). To further increase

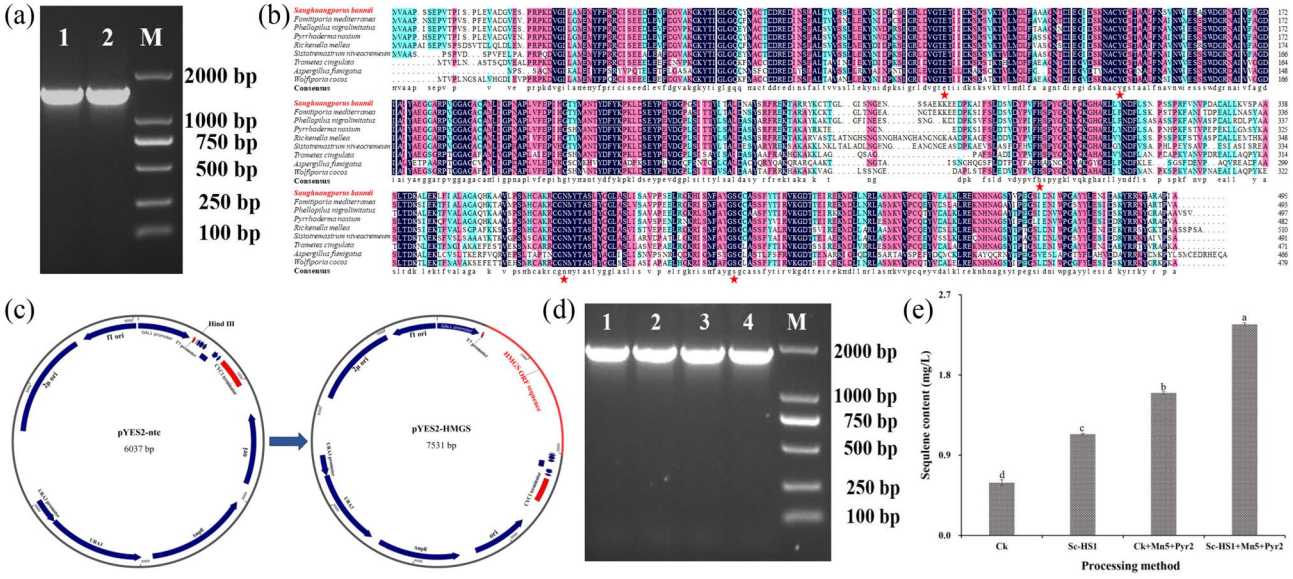

Fig. 4 Functional analysis of *HMGS* from *S. baumii*. **a** *HMGS* cloning. **b** Sequence alignment of nine amino acid residues of HMGS, highlighting five conserved amino acid residues (Glu, Tyr, His, Asn, and Ser) marked with pentagrams. **c** Schematic representation of the *HMGS* overexpression vector construction process. **d** Identification of positive clones. **e** Squalene content in *S. cerevisiae*

squalene production, supplementing the fermentation medium with 5 mM Mn^{2+} and 2 mg/L pyruvate (Fig. S4) increased squalene content to 1.6 ± 0.01 mg/L in the Ck group. The introduction of the Sc-HS1 with 5 mM Mn^{2+} and 2 mg/L pyruvate further boosted squalene content to 2.37 ± 0.02 mg/L (Fig. 4e), confirming the key regulatory role of *HMGS* in triterpenoid biosynthesis in *S. baumii*.

Discussion

Exogenous inducers have been reported to positively influence the growth and development of macrofungi, as well as the production of metabolites [9, 15, 18]. Herein 1 mM Mn^{2+} was found to significantly promote mycelial biomass accumulation, which is essential for the large-scale production of bioactive compounds [19]. This effect was likely due to the upregulation of the expression of genes involved in starch and sucrose metabolism, causing a substantial increase in soluble sugar content (6.23 ± 0.06 mg/g) compared to the Mn0 group (6.03 ± 0.08 mg/g, Fig. S5) and leading to the generation of sufficient energy for mycelial growth [20].

In contrast, treatment with 10 mM Mn^{2+} significantly inhibited *S. baumii* mycelial biomass accumulation, negatively impacting bioactive compound production in industrial-scale bioprocessing. This growth inhibition likely stems from Mn^{2+}-induced up-regulation of *SOD2* in the peroxisomal pathway, resulting in the insufficient removal of H_2O_2, a cytotoxic byproduct (Fig. S6). H_2O_2 accumulation has been reported to lead to toxicity in *S. baumii* mycelia [21]. Nevertheless, 10 mM Mn^{2+} significantly increased total triterpenoids content, even though it suppressed biomass production. This promotion likely arises from Mn^{2+}-induced up-regulation of *HMGS* within the terpenoid biosynthesis pathway. *HMGS* has long been recognized as crucial for triterpenoid biosynthesis. Its expression is a major determinant of final triterpenoids yield [16, 22]. We found that *HMGS* in *S. baumii* contains a conserved HMG-CoA-S_euk domain, along with five highly conserved amino acid residues, which are essential for HMG-CoA synthase activity and its role in catalyzing the conversion of acetyl-CoA to HMG-CoA [23].

The heterologous expression of *HMGS* in *S. cerevisiae* has been found to enhance triterpenoids content. Our results also indicate that Mn^{2+} and pyruvate, either individually or in combination, increased squalene content, with the combined induction proving particularly effective (Fig. S4, Fig. 4e). The introduction of key genes involved in triterpenoid biosynthesis, coupled with inducers (supplementing the Mn^{2+} and pyruvate in the medium), represents a promising strategy for enhancing triterpenoids accumulation. These findings provide valuable insights for the large-scale biotechnological production of triterpenoids.

Conclusion

Our findings confirm the bidirectional effects of Mn^{2+} on *S. baumii* growth, development, and metabolites production. Specifically, 1 mM Mn^{2+} significantly enhanced mycelial biomass accumulation, likely due to the stimulation of soluble sugar accumulation and the upregulation of the expression of metabolic genes, which provided sufficient energy for mycelial growth. Although 10 mM Mn^{2+} inhibited mycelial biomass accumulation and induced toxicity, total triterpenoids accumulation was

significantly promoted. Notably, *HMGS* expression was upregulated. The heterologous expression of *HMGS* confirmed its role as a functional enzyme essential for triterpenoid biosynthesis, facilitating squalene accumulation. Furthermore, the combined addition of Mn^{2+} and pyruvate was the most effective strategy for enhancing squalene production. These findings provide critical insights into the metabolic regulation of triterpenoid biosynthesis in *S. baumii* and lay the groundwork for optimizing triterpenoids production through metabolic engineering.

Materials and methods

Fungal strain and vector information

S. baumii fruiting body was collected from the living trunk of *Syringa reticulata* in Liangshui Nature Reserve, Yichun, Heilongjiang, China. Mycelia were isolated from the fruiting body using a tissue separation method and identified via internal transcribed spacer ITS region sequencing for both *S. baumii* fruiting body and mycelia. *Escherichia coli* DH5α and *S. cerevisiae* INVSc1 competent cells were purchased from WEIDI Biotechnology Co., Ltd. (Shanghai, China). The pYES2-ntc vector was stored in the Forestry Protection Laboratory of Northeast Forestry University.

Mn^{2+} treatment of *S. baumii* mycelia

Mycelial cakes (1 cm in diameter) of *S. baumii* were inoculated into PD medium and incubated at 25 °C for 10 days to obtain a mycelial culture. This culture was then homogenized to prepare a liquid seed culture, which was inoculated into 250 mL PD medium at a 4% (v/v) inoculum concentration, followed by incubation at 25 °C with shaking at 180 rpm for an additional 8 days. Sterile $MnCl_2$ solution was then added to the PD medium to achieve final concentrations of 0.5 mM (Mn0.5 group), 1 mM (Mn1 group), 5 mM (Mn5 group), 10 mM (Mn10 group), and 50 mM (Mn50 group) [18]. The Mn0 group was treated with sterile water as a control. Cultivation continued for an additional 2 days, after which *S. baumii* mycelia were harvested for biomass measurement, metabolite analyses, and transcriptome profiling.

Determination of *S. baumii* biomass and triterpenoids content

S. baumii mycelia treated with different Mn^{2+} concentrations were harvested and dried in an oven at 45 °C until a constant weight was achieved. The biomass of samples from the Mn0.5, Mn1, Mn5, Mn10, and Mn50 groups was then measured. Total triterpenoids content was determined through spectrophotometry. Specifically, 0.1 g of *S. baumii* powder was suspended in 2 mL of 60% (v/v) ethanol, and then placed in an ultrasonic chamber for 30 min at 100 W (40 kHz); paused for 1 min, the ultrasound treatment was repeated. Afterwards, the mixture is then centrifuged at 13,000×g for 5 min to remove mycelial debris, and the supernatant was dried at 70℃ in a thermostatic water bath. The residues were reacted with vanillin–acetic acid, perchloric acid, and other reagents. Absorbance was measured at 551 nm, and total triterpenoids content was finally calculated [24, 25].

Transcriptome sequencing and qRT-PCR validation

Samples of *S. baumii* treated with Mn^{2+}, showing significant differences in triterpenoids content, were selected for transcriptome analysis. Transcriptome sequencing was performed using the Illumina HiSeq 2500 platform at PANOMIX Biomedical Tech Co., Ltd. (Suzhou, China). Raw sequencing reads were processed to obtain high-quality transcript sequences, with the longest transcript from each cluster designated as a unigene. These unigenes were annotated, and FPKM (Fragments Per Kilobase Million) values were calculated. Principal component analysis (PCA) was performed to assess expression levels across samples. Differentially expressed genes (DEGs) were identified using a threshold of $|\log_2 \text{fold-change}| > 1$ and $p < 0.05$. Clustering analysis and KEGG pathway enrichment analysis of DEGs were also conducted. To validate the sequencing results, nine DEGs were selected for qRT-PCR, ensuring consistency with transcriptomic data [26].

Quantification of acetyl-CoA, soluble sugar, and hydrogen peroxide (H_2O_2) levels

Acetyl-CoA content was measured using the ACA-2 A-Y kit (Suzhou Comin, Suzhou, China). Briefly, 0.1 g of pulverized *S. baumii* sample was homogenized in 1 mL of Tris-HCl buffer on ice. The homogenate was then centrifuged at 4 °C, and the supernatant thus obtained was used for subsequent assay reactions. Absorbance was measured at 340 nm to determine acetyl-CoA content. Soluble sugar content was measured using the KT-2-Y kit (Suzhou Comin). Briefly, 0.1 g of pulverized *S. baumii* sample was homogenized in 1 mL of distilled water. The homogenate was then incubated in a 95 °C water bath, followed by centrifugation at 25 °C. The supernatant thus obtained was used for subsequent measurements. Absorbance was measured at 620 nm to determine soluble sugar content. H_2O_2 content was determined using the H_2O_2 –2-Y kit (Suzhou Comin). Briefly, 0.1 g of pulverized *S. baumii* sample was homogenized in 1 mL of acetone on ice, followed by centrifugation at 4 °C. The supernatant thus obtained was used for subsequent assay reactions. Absorbance was measured at 415 nm to quantify H_2O_2 content.

Identification and functional analysis of key genes involved in triterpenoid biosynthesis in *S. baumii*

Based on transcriptomic data, Pearson correlation analysis was performed to analyze the relationship between triterpenoid biosynthesis-related gene expression and total triterpenoids/acetyl-CoA content. DEGs that were positively correlated with triterpenoid biosynthesis and exhibited a significant fold change were selected as candidate target genes. The target gene was amplified via PCR using the pYE-HMGS-F/-R primers (Table S1), with cDNA as the template. The amplicons were subsequently sequenced (Sangon, Shanghai, China). Target gene fragments with correct sequencing results were cloned into the pYES2-ntc vector and transformed into *E. coli* DH5α and *S. cerevisiae* INVSc1 competent cells. Positive transformants were identified using the T7F and C1R primers (Table S1). Induction experiments were conducted using the positive *S. cerevisiae* transformants to evaluate squalene content [27, 28]. *S. cerevisiae* harboring the empty pYES2-ntc vector was used as the control (Ck) group. The ability of the target gene to regulate triterpenoid biosynthesis was assessed by comparing squalene content between the target gene-expressing group and the Ck group.

Data analysis

All data, including biomass, triterpenoids content, acetyl-CoA content, soluble sugar content, H_2O_2 content, and transcriptome analysis, were obtained from three biological replicates. Statistical significance was assessed using Duncan's test ($p < 0.05$) with SPSS software v17.0 (SPSS Inc., Chicago, IL, USA). Pearson correlation analysis was conducted to determine the relationship between gene expression levels and acetyl-CoA/total triterpenoids content.

Abbreviations

S. baumii	*Sanghuangporus baumii*
S. cerevisiae	*Saccharomyces cerevisiae*
ITS	Internal Transcribed Spacer
H_2O_2	Hydrogen peroxide
FPKM	Fragments Per Kilobase Million
PCA	Principal Component Analysis
DEGs	Differentially expressed genes

Supplementary Information

The online version contains supplementary material available at https://doi.org/10.1186/s12870-025-07200-7.

Supplementary Material 1: Table S1. Primers used for qRT-PCR. Table S2: RNA-Seq data statistics of *S. baumii*. Table S3: Transcript abundance of relevant genes based on *S. baumii* transcriptome data annotation.

Supplementary Material 2: Fig. S1. Comparison of ITS sequences of *S. baumii* fruiting body and mycelia. Fig. S2: Sequencing saturation analysis of *S. baumii* samples treated with different Mn^{2+} concentrations. Fig. S3: Conservative domain analysis of *HMGS* from *S. baumii*. Fig. S4: Squalene content in *S. cerevisiae* harboring the pYES2-ntc vector under treatment with exogenous inducers. (a) *S. cerevisiae* treated with different Mn^{2+} and (b)pyruvate concentrations. Fig. S5: Changes in the starch and sucrose metabolism pathway of *S. baumii* under Mn^{2+} treatment. (a) Expression levels of related genes. (b) Soluble sugar content. Fig. S6: Changes in the peroxisome pathway of *S. baumii* under Mn^{2+} treatment. (a) Expression levels of related genes. (b) H_2O_2 content.

Acknowledgements

Not applicable.

Authors' contributions

Z. L. designed the project and wrote the manuscript. C. S. and W. X. performed the experiments. A. W. collected and analyzed the data. L. Z. revised the manuscript. All authors have approved the final manuscript.

Funding

This work was supported by the National Natural Science Foundation of China (32301597), and the Postdoctoral research project of Heilongjiang Province (LBH-Z23003).

Data availability

All data generated or analysed during this study are included in this article and supplementary materials. *HMGS* (PX056318) and ITS (PX054576) sequencing data are stored in the NCBI database. All materials are available through corresponding authors upon reasonable request.

Declarations

Ethics approval and consent to participate

experimental research on fungi in this study complied with institutional, national, or international guidelines and legislation.

Consent for publication

Not applicable.

Competing interests

The authors declare no competing interests.

Received: 13 March 2025 / Accepted: 7 August 2025
Published online: 28 August 2025

References

1. Hao Z, Liu Y, Guan W, Pan J, Li MM, Wu J, Liu Y, Kuang H, Yang B. *Syringa reticulata* potently inhibits the activity of SARS-CoV-2 3CL protease. Biochem Biophys Rep. 2024;37: 101626.
2. Shen S, Liu SL, Jiang JH, Zhou LW. Addressing widespread misidentifications of traditional medicinal mushrooms in *Sanghuangporus* (Basidiomycota) through ITS barcoding and designation of reference sequences. IMA Fungus. 2021;12:10.
3. Liu X, Cui S, Dan C, Li W, Xie H, Li C, Shi L. *Phellinus baumii* polyphenol: a potential therapeutic candidate against lung cancer cells. Int J Mol Sci. 2022;23(24): 16141.
4. Zheng N, Ming Y, Chu J, Yang S, Wu G, Li W, Zhang R, Cheng X. Optimization of extraction process and the antioxidant activity of phenolics from *Sanghuangporus baumii*. Molecules. 2021;26(13):3850.
5. Hwang HJ, Kim SW, Lim JM, Joo JH, Kim HO, Kim HM, Yun JW. Hypoglycemic effect of crude exopolysaccharides produced by a medicinal mushroom *Phellinus baumii* in streptozotocin-induced diabetic rats. Life Sci. 2005;76(26):3069–80.
6. Fu L, Song J, Lu N, Yan J, Lin J, Wang W. Effects of cultivation methods on the nutritional content, active component content, and antioxidant activity of fruiting bodies of *Sanghuangporus baumii* (Agaricomycetes). Int J Med Mushrooms. 2023;25(7):45–54.
7. Shao Y, Guo H, Zhang J, Liu H, Wang K, Zuo S, Xu P, Xia Z, Zhou Q, Zhang H, et al. The genome of the medicinal macrofungus *Sanghuang* provides insights into the synthesis of diverse secondary metabolites. Front Microbiol. 2020;10:3035.

8. Liu Z, Liu R, Zou L. Development of a transformation system for the medicinal fungus *Sanghuangporus baumii* and acquisition of high-value strain. Mycobiology. 2023;51(3):169–77.
9. Huang J, Li MT, Shen AQ, Wan X, Liu XQ, Li YZ, Yang QQ, Zhang BB. The mechanistic study of adding polyunsaturated fatty acid to promote triterpenoids production in submerged fermentation of *Sanghuangporus baumii*. Biochem Eng J. 2023;191: 108800.
10. Mori K, Aki S, Kido M. Synthesis of new terpene skeletons by chemical cyclization of epoxy olefins. Bull Soc Chim Belg. 1994;1994(4):319–24.
11. Franziska R, Philipp H. Taxane Meets propellane: first chemical synthesis of highly complex diterpene Canataxpropellane. Angew Che Int Ed. 2020;59(26):10232–4.
12. Wang YS, Xu YJ, Gao LP, Yu O, Wang XZ, He XJ, Jiang XL, Liu YJ, Xia T. Functional analysis of flavonoid 3′,5′-hydroxylase from tea plant (*Camellia sinensis*): critical role in the accumulation of catechins. BMC Plant Biol. 2014;14:347.
13. Wang S, Meng D, Feng M, Li C, Wang Y. Efficient plant triterpenoids synthesis in *Saccharomyces cerevisiae*: from mechanisms to engineering strategies. ACS Synth Biol. 2024;13(4):1059–76.
14. Wang S, Li J, Fan Q, Wang S, Sun C, Yan M. Transcriptome analysis of *Ganoderma Lingzhi* liquid fermentation process using corn straw as matrix. Agriculture. 2024;14(8):1271.
15. Ren A, Qin L, Shi L, Dong X, Mu DS, Li YX, Zhao MW. Methyl jasmonate induces Ganoderic acid biosynthesis in the basidiomycetous fungus *Ganoderma lucidum*. Bioresour Technol. 2010;101(17):6785–90.
16. Ren A, Ouyang X, Shi L, Jiang AL, Mu DS, Li MJ, Han Q, Zhao MW. Molecular characterization and expression analysis of *GlHMGS*, a gene encoding hydroxymethylglutaryl-CoA synthase from *Ganoderma lucidum* (Ling-zhi) in Ganoderic acid biosynthesis pathway. World J Microbiol Biotechnol. 2013;29(3):523–31.
17. Zhang G, Cao Q, Liu J, Liu B, Li J, Li C. Refactoring β-amyrin synthesis in *Saccharomyces cerevisiae*. AIChE J. 2015;61(10):3172–9.
18. Xu YN, Xia XX, Zhong JJ. Induction of ganoderic acid biosynthesis by Mn^{2+} in static liquid cultivation of *Ganoderma lucidum*. Biotechnol Bioeng. 2014;111(11):2358–65.
19. Hu YH, Ge MD, Sun DN, Chen L, Cheung PCK, You CP, Chen XZ, Sun MX, Ng H. Stimulating mechanism of corn oil on biomass and polysaccharide production of *Pleurotus tuber*-regium mycelium. Int J Biol Macromol. 2021;201:93–103.
20. Hsu FL, Chen HC, Lu MK. Polysaccharides from *Cunninghamia Konishii* promote the mycelial growth of *Antrodia cinnamomea*. Food Hydrocolloid. 2016;53:2–6.
21. Aguirre J, Hansberg W, Navarro R. Fungal responses to reactive oxygen species. Med Mycol. 2006;44(Suppl):S101-7.
22. Wang H, Nagegowda DA, Rawat R, Bouvier-Nave P, Guo DJ, Bach TJ, Chye ML. Overexpression of *Brassica juncea* wild-type and mutant HMG-CoA synthase 1 in *Arabidopsis* up-regulates genes in sterol biosynthesis and enhances sterol production and stress tolerance. Plant Biotechnol J. 2012;10:31–42.
23. Campobasso N, Patel M, Wilding IE, Kallender H, Rosenberg M, Gwynn MN. *Staphylococcus aureus* 3-hydroxy-3-methylglutaryl-CoA synthase: crystal structure and mechanism. J Biol Chem. 2004;279:44883–8.
24. Sun TT, Zou L, Zhang LF, Zhang J, Wang XT. Methyl jasmonate induces triterpenoid biosynthesis in *Inonotus baumii*. Biotechnol Biotechnol Equip. 2017;31(2):312–7.
25. Chen D, Chen X, Zheng X, Zhu J, Xue T. Combined metabolomic and transcriptomic analysis reveals the key genes for triterpenoid biosynthesis in *Cyclocarya paliurus*. BMC Genomics. 2024;25(1):1197.
26. Livak KJ, Schmittgen TD. Analysis of relative gene expression data using real-time quantitative PCR and the $2^{-\Delta\Delta CT}$ method. Methods. 2001;25:402–8.
27. Sedbare R, Raudone L, Zvikas V, Viskelis J, Liaudanskas M, Janulis V. Development and validation of the UPLC-DAD methodology for the detection of triterpenoids and phytosterols in fruit samples of *Vaccinium macrocarpon* Aiton and *Vaccinium oxycoccos* L. Molecules. 2022;27:4403.
28. Salvo A, Torre GLL, Stefano VD, Capocchiano V, Mangano V, Saija E, Pellizzeri V, Casale KE, Dugo G. Fast UPLC/PDA determination of squalene in Sicilian P.D.O. Pistachio from bronte: optimization of oil extraction method and analytical characterization. Food Chem. 2017;221:1631–6.

Publisher's note